

**Early results from the BRAHMS experiments at RHIC:  
Pseudorapidity distributions of charged particles from Au + Au  
collisions at  $\sqrt{s_{NN}} = 130$  GeV and 200 GeV<sup>1</sup>**

**Zbigniew Majka<sup>4</sup> ( for BRAHMS Colaboration)**

I. G. Bearden<sup>7</sup>, D. Beavis<sup>1</sup>, C. Besliu<sup>10</sup>, Y. Blyakhman<sup>6</sup>, Budick<sup>6</sup>, H. Bøggild<sup>7</sup>, C. Chasman<sup>1</sup>, C. H. Christensen<sup>7</sup>, P. Christiansen<sup>7</sup>, J. Cibor<sup>3</sup>, R. Debbe<sup>1</sup>, E. Enger<sup>12</sup>, J. J. Gaardhøje<sup>7</sup>, K. Hagel<sup>8</sup>, O. Hansen<sup>7</sup>, A. Holm<sup>7</sup>, A. K. Holme<sup>12</sup>, H. Ito<sup>11</sup>, E. Jakobsen<sup>7</sup>, A. Jipa<sup>10</sup>, J. I. Jørdre<sup>9</sup>, F. Jundt<sup>2</sup>, C. E. Jørgensen<sup>7</sup>, R. Karabowicz<sup>4</sup>, T. Keutgen<sup>8</sup>, E. J. Kim<sup>1,5</sup>, T. Kozik<sup>4</sup>, T. M. Larsen<sup>12</sup>, J. H. Lee<sup>1</sup>, Y. K. Lee<sup>5</sup>, G. Løvholden<sup>12</sup>, Z. Majka<sup>4</sup>, A. Makeev<sup>8</sup>, B. McBreen<sup>1</sup>, M. Mikelsen<sup>12</sup>, M. Murray<sup>8</sup>, J. Natowitz<sup>8</sup>, B. S. Nielsen<sup>7</sup>, J. Norris<sup>11</sup>, K. Olchanski<sup>1</sup>, J. Olness<sup>1</sup>, E. K. Olsen<sup>7</sup>, D. Ouerdane<sup>7</sup>, R. Planeta<sup>4</sup>, F. Rami<sup>2</sup>, D. Röhrich<sup>9</sup>, B. H. Samset<sup>12</sup>, D. Sandberg<sup>7</sup>, S. J. Sanders<sup>11</sup>, R. A. Scheetz<sup>1</sup>, P. Staszal<sup>7</sup>, T. F. Thorsteinsen<sup>9+</sup>, T. S. Tveter<sup>12</sup>, F. Videbæk<sup>1</sup>, R. Wada<sup>8</sup>, A. Wieloch<sup>4</sup>, and I. S. Zgura<sup>10</sup>

1. Brookhaven National Laboratory, New York, 11973, USA.
  2. Institut de Recherches Subatomiques and Université Louis Pasteur, Strasbourg, France.
  3. H. Niewodniczanski Institute of Nuclear Physics, Kraków, Poland.
  4. M. Smoluchowski Institute of Physics, Jagiellonian University, Kraków, Poland.
  5. Johns Hopkins University, Baltimore, Maryland 21218, USA.
  6. New York University, New York, New York 10003, USA.
  7. Niels Bohr Institute, University of Copenhagen, Denmark
  8. Cyclotron Institute, Texas A&M University, College Station, Texas 77843, USA.
  9. University of Bergen, Department of Physics, Bergen, Norway.
  10. University of Bucharest, Romania.
  11. University of Kansas, Lawrence, Kansas 66045, USA.
  12. University of Oslo, Department of Physics, Oslo, Norway.
- + Deceased

**Abstract**

We describe the general motivation and detector layout for the BRAHMS experiment at RHIC. BRAHMS is designed to study the properties of strongly interacting matter by precise measurements of charged hadrons produced in ultra-relativistic collisions. In addition to an overview of the experiment, this talk presents early results on charged particle densities as a function of pseudo-rapidity and collision centrality for the  $^{197}\text{Au} + ^{197}\text{Au}$  reaction at  $\sqrt{s_{NN}} = 130$  GeV and 200 GeV. Several models that have been developed in anticipation of the RHIC results are compared to the data.

---

<sup>1</sup> Presented at the XL International Winter Meeting on Nuclear Physics, Bormio (Italy) January 21–26, 2002.

## 1. Introduction

By colliding heavy ions at high energies one can create hadronic matter at high energy densities. At the energy of 1 AGeV, which is available at SIS (GSI, Darmstadt), the nuclei are stopped, compressed and moderately heated. At the energies reached by the AGS (Brookhaven National Laboratory) and SPS (CERN) facilities, where heavy nuclei have been accelerated up to 17 AGeV and 160 AGeV, respectively, even higher temperatures have been obtained. However, at such energies the colliding nuclei are no longer completely stopped and the baryon chemical potential of the matter created decreases. The theory of strong interactions, QCD (Quantum Chromodynamics), predicts a phase transition to a quark-gluon plasma (QGP) at high energy densities for strongly interacting bulk matter. The critical energy density is on the order of  $1 \text{ GeV/fm}^3$  and can be reached, for instance, by heating hadronic matter at zero net baryon density to a temperature of about 160 MeV or by compressing cold matter to the baryon density above 3 times of the equilibrium density.

On Feb. 10, 2000, CERN announced [1], "Evidence for New State of Matter: An Assessment of the results from the CERN Lead Beam Programme". Five months later, the Relativistic Heavy Ion Collider (RHIC) started its operation at Brookhaven National Laboratory, heralding a new era of systematic studies of strongly interacting matter. These studies will eventually lead to a quantitative understanding of "bulk QCD".

RHIC has two beams circulating in opposite directions around a ring with six interaction regions [2]. Four of these regions are instrumented with the experimental setups of BRAHMS, PHENIX, PHOBOS and STAR. The accelerator has a design luminosity of  $2 \times 10^{26} \text{ cm}^{-2} \text{ s}^{-1}$  for Au + Au beams at  $\sqrt{s_{NN}} = 200 \text{ GeV}$  and produces collisions at a rate up to 1,000 Hz.

## 2. BRAHMS Physics Goals

The Broad Range Hadron Magnetic Spectrometers (BRAHMS) experimental setup is designed to study the basic reaction mechanisms in ultra-relativistic heavy ion collisions by measuring momentum spectra and yields for charged hadrons over a wide range of transverse momenta and rapidity. BRAHMS achieves particle identification for  $p$ ,  $\pi$  and  $K$  at rapidities with  $0 < y < 4$  and transverse momenta with  $0.2 \text{ GeV}/c < p_t < 4 \text{ GeV}/c$  for all energies and beams available at RHIC. At forward angles this  $p_t$  range translates into large momenta up to 30 GeV/c.

The particle spectral shapes and their dependence on rapidity reveal the reaction dynamics and degree of thermalization attained. The high transverse momentum parts of the spectra carry information from the early phase of the reaction. The yields as a function of rapidity are important indicators of densities reached in the collisions and of the entropy produced. Determination of the collision centrality is an integral part of the measurements.

The BRAHMS physics program will address the following topics:

?? Reaction mechanism

?? Stopping

- ? ? Chemical equilibrium
- ? ? Thermalization
- ? ? Baryo-chemical potential
- ? ? Particle production and particle to anti-particle ratios
- ? ? Strangeness production
- ? ? Mini-jet production systematic

The extended phase-space coverage of BRAHMS will allow investigation of a number of these topics in a manner that complements results of the other RHIC experiments.

### 3. BRAHMS Experimental Layout

The very different momenta and particle densities at mid-rapidity and forward angles has led to a design with two moveable magnetic spectrometers [3]. The BRAHMS experiment also has four global detector systems. A perspective view of the experimental setup is presented in Figure 1.

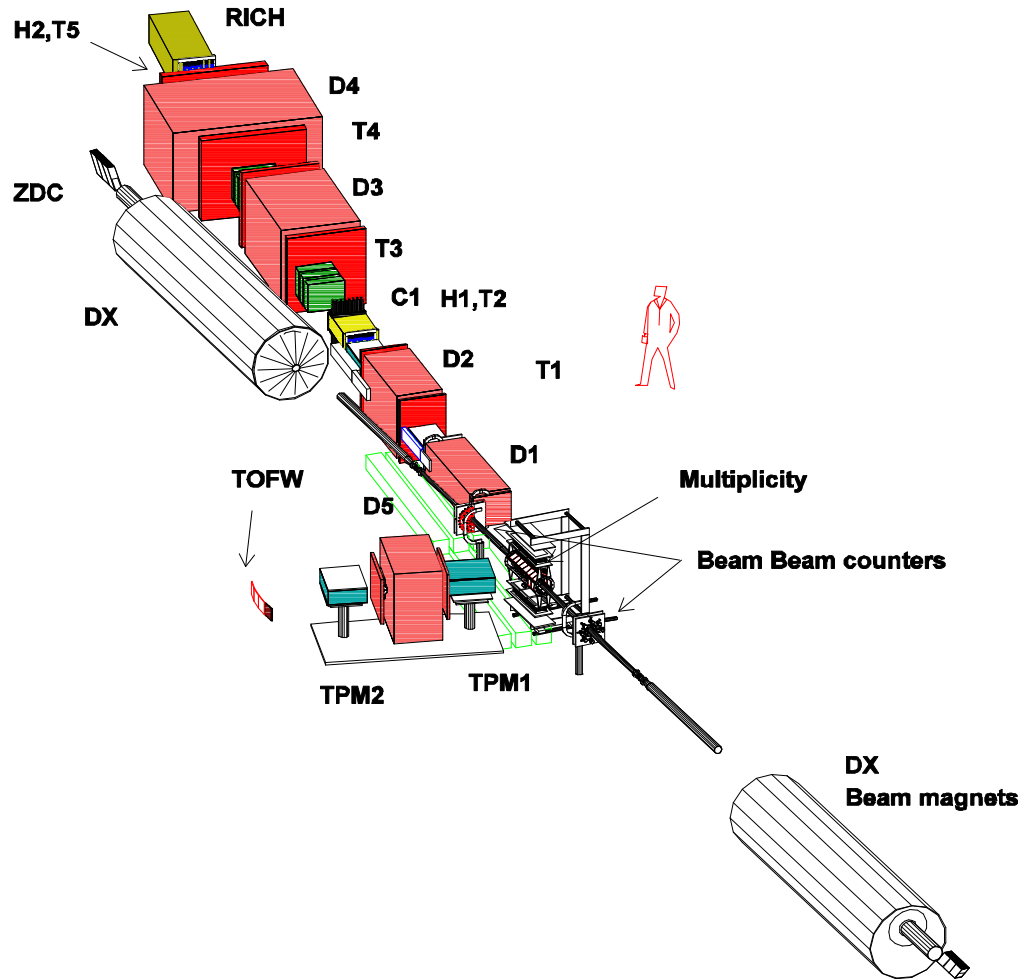


Figure 1. The BRAHMS experimental setup in perspective.

The Forward Spectrometer (FS) has a solid angle of 0.8 msr and measures identified particles having momenta up to 25 GeV/c in the angular range of  $2.3^\circ < \theta < 30^\circ$ . Four magnets (D1 - D4) are used for sweeping and analyzing particles emerging from the reaction. The forward arm of the FS tracking detectors (T1 and T2) are Time Projection Chambers (TPCs) which provide good three-dimensional track recognition and rejection of background in a high multiplicity environment. The back arm of the FS tracking detectors (T3-T5) are Drift Chambers (DCs) and each consists of three identical modules that contain 10 (8) detection planes for T3 (T4-T5). Particle identification in the FS is based on two time of flight hodoscopes (H1-H2) as well as on Cerenkov measurements. H1 and H2 consist of 40 and 32 slats of plastic scintillator slats, respectively with each slat instrumented with two phototubes, one on either end. H1 and H2 are positioned 9m and 20m from the nominal vertex, respectively. Higher momentum particles are identified with a threshold Cerenkov detector (C1) placed behind D2 magnet and a ring imaging Cerenkov detector (RICH) placed behind H2.

The Mid-Rapidity Spectrometer (MRS) has a solid angle of 6.5 msr and measures identified particles having momenta in the range  $0.2 \text{ GeV}/c < p < 5 \text{ GeV}/c$  in the angular range of  $30^\circ < \theta < 95^\circ$ . The single dipole magnet (D5) of the MRS is placed between two TPC's which are used for tracking. Particle identification is obtained with a time of flight wall.

Four global detector systems are used to enable event characterization:

?? Around the interaction vertex is a global multiplicity array to estimate event-by-event centrality. The Multiplicity Array (MA) consists of two independent systems with a modestly segmented silicon strip detector array (SiMA) surrounded by an outer plastic scintillator tile array (TMA) in a double, hexagonal-side barrel arrangement. The silicon strip detectors also provide information on overall charged particle yields, with an effective coverage in pseudorapidity of  $-3.0 < \eta < 3.0$ .

?? Beam - Beam Counters (BBC) are located 220 cm from the nominal interaction vertex near the beam pipe. They are constructed from two sizes of Cerenkov radiators glued to photo-multiplier tubes. The primary task for the BB counters is to provide a start time and a level 0 trigger. The 50 ps time resolution of the array allows determination of the vertex position to an accuracy of 0.9 cm. These detectors also provide multiplicity information at high pseudo-rapidity with  $2.1 < \eta < 4.7$ .

?? The Zero Degree Calorimeters (ZDCs) are located 18 m from the nominal interaction vertex and detect neutrons emitted in a small cone ( $\theta < 2 \text{ mrad}$ ) around the downstream beam directions. The neutron multiplicity is correlated with event geometry and can therefore be used along with the multiplicity array and beam-beam counters to estimate the centrality of the collision. The ZDCs coincidence can provide a minimum-bias selection making it useful as an event trigger as well as a luminosity monitor. Clean selection of minimum-biased events required a coincidence between the two ZDCs and a minimum of 4 hits in the TMA. Such selections include 95% of the total nuclear cross section of 7.1 b. There are identical sets of ZDCs in all of the RHIC experiments. This enables a cross check of results from all four experiments and provides luminosity measurements for the RHIC machine group.

The BRAHMS Data Acquisition is based on a distributed system of loosely coupled front-end processors that are interrupted by actions of trigger systems and a high-end workstation that serves the function of event builder and user run-control. The front-end VME processors initiates and interrupts the readout of data from the crates. The event fragments are buffered in local memory and transferred via 100M-bit Ethernet to a high end Unix server. The event builder program assembles a complete event. The server has a disk spool area capable of holding up to 100 Gb of data and acting as a buffer for the raw data files before they are sent using the pftp protocol on a gigabit link to the HPSS storage at the RHIC Computing Facility. A close to on-line analysis of the data in the disk spool area is possible using the NFS protocol.

#### 4. Measurements and results

There have so far been two extended periods of data taking at RHIC. The 2000 running period with Au + Au collisions at  $\sqrt{s_{NN}} = 130$  GeV enabled BRAHMS to record a significant dataset that has led to two publications (see Ref. [4] and [5]). For this run period, the MRS recorded data at the angle settings of 90, 45 and 40 degrees with two field settings and with both field polarities at each setting. The FS was operated at an angle of 8 degrees with one magnetic field setting and both field polarities. The data were analyzed yielding physics results for charged particle densities and for rapidity dependence of particle ratios. In the second run period 2001/2002, the primary physics goal for BRAHMS was to study charged particle production, particle ratios and momentum spectra for Au + Au collisions at  $\sqrt{s_{NN}} = 200$  GeV. The collected data are currently being analyzed, with the first results on the pseudorapidity distributions of charged particles having been submitted for publication [6].

The present talk summarizes the BRAHMS Collaboration investigations of multiplicity distributions of emitted charged particles in relativistic collisions between  $^{197}\text{Au}$  nuclei at RHIC energies. The results on the particle ratios are presented by D. Ouerdane [7] in this volume.

Pseudorapidity distributions of emitted charged particles,  $dN_{ch}/d\eta$ , is a fundamental observable in ultra-relativistic collisions. The particle densities are sensitive to the relative contributions of soft and hard processes. The total number of charged particles and the angular dependence of the charged particle distributions are dependent on the amount of hadronic re-scattering, the degree of chemical and thermal equilibration and role of subatomic processes. The pseudorapidity distributions were investigated as a function of collision centrality. Because the collision centrality can be related to the number of participant nucleons in the reaction, different systems can be compared based on simple nucleon-nucleon superposition models. Reaction centrality was determined by selecting different regions of the total multiplicity distribution measured in either the MA or BBC detectors.

Table 1 presents the charged particle densities as a function of centrality and pseudo-rapidity measured for Au + Au collisions at  $\sqrt{s_{NN}} = 130$  GeV (regular characters) and  $\sqrt{s_{NN}} = 200$  GeV (bold characters). One can see that charged particle densities are considerably higher at  $\sqrt{s_{NN}} = 200$  GeV as compared to the collisions at  $\sqrt{s_{NN}} = 130$  GeV. This table also presents the integrated charged-particle multiplicities in the range  $-4.7 \leq \eta \leq 4.7$  and the number of participating

**Table 1**

Centrality [%]	$\sqrt{s} = 0$	$\sqrt{s} = 1.5$	$\sqrt{s} = 3.0$	$\sqrt{s} = 4.5$	$N_{ch}$	$N_{part}$
0 – 5	553 ? 36	554 ? 37	372 ? 37	107 ? 15	3860 ? 300	352
	<b>625 ? 55</b>	<b>627 ? 54</b>	<b>470 ? 44</b>	<b>181 ? 22</b>	<b>4630 ? 370</b>	<b>357</b>
5 – 10	447 ? 29	454 ? 31	312 ? 36	94 ? 13	3180 ? 250	299
	<b>501 ? 44</b>	<b>515 ? 48</b>	<b>397 ? 37</b>	<b>156 ? 18</b>	<b>3810 ? 300</b>	<b>306</b>
10 – 20	345 ? 23	348 ? 25	243 ? 27	79 ? 10	2470 ? 190	235
	<b>377 ? 33</b>	<b>386 ? 35</b>	<b>309 ? 28</b>	<b>125 ? 14</b>	<b>2920 ? 230</b>	<b>239</b>
20 – 30	237 ? 16	239 ? 16	172 ? 18	59 ? 8	1720 ? 130	165
	<b>257 ? 23</b>	<b>267 ? 23</b>	<b>216 ? 17</b>	<b>90 ? 10</b>	<b>2020 ? 160</b>	<b>168</b>
30 – 40	156 ? 11	159 ? 11	117 ? 13	43 ? 6	1160 ? 90	114
	<b>174 ? 16</b>	<b>182 ? 16</b>	<b>149 ? 14</b>	<b>64 ? 7</b>	<b>1380 ? 110</b>	<b>114</b>
40 – 50	98 ? 7	104 ? 7	77 ? 9	30 ? 4	750 ? 60	75
	<b>110 ? 10</b>	<b>115 ? 11</b>	<b>95 ? 9</b>	<b>43 ? 5</b>	<b>890 ? 70</b>	<b>73</b>

baryons estimated using the HIJING model [8]. For the most central collisions, the charged particle densities per participating baryon pair is equal to  $3.5 \pm 0.3$  at  $\sqrt{s}_{NN} = 200$  GeV and indicates a (11 $\pm$ 1)% increase relative to the value obtained at the lower beam energy. For the most peripheral collisions presented here at  $\sqrt{s}_{NN} = 200$  GeV and at  $\sqrt{s} = 0$ , the particle density scaled to the number of participating pairs is equal  $3.0 \pm 0.3$ . An increase of the integrated multiplicity by (21 $\pm$ 1)% is observed in the considered collision energy range for the most central collisions.

Theoretical model predictions have been compared to the measured  $dN_{ch}/d\eta$  distributions for selected centrality ranges (0-5%, 5-10%, 20-30% and 40-50%). The AMPT model [9] which is a cascade model based on HIJING but including final state re-scattering of produced particles is able to reproduce the general trend of measured distributions at both RHIC energies. Calculations of Kharzeev and Levin [10], which are based on classical QCD, also describe the data well. On the other hand, the UrQMD transport model [11] considerably overestimates the particle production rates at RHIC energies.

The ratio of the pseudo-rapidity densities measured at  $\sqrt{s}_{NN} = 130$  GeV and  $\sqrt{s}_{NN} = 200$  GeV for different centralities shows an increase of between 10% and 20 % in charged particle density as a function of energy for a central plateau region ( $\eta < 2.5$ ). The increase in this ratio observed at the forward rapidities (see Table 1) is due to the widening of the multiplicity distribution at higher energy, consistent with the increase in beam rapidity.

Figure 2 shows the charged particle densities normalized to the number of participant pairs for the (0 – 5)% central collisions (open circles at  $\sqrt{s_{NN}} = 200$  GeV and closed circles at  $\sqrt{s_{NN}} = 130$  GeV) and for the (40 – 50)% central collisions at  $\sqrt{s_{NN}} = 200$  GeV (open squares). Results obtained at CERN-SPS for the 9.4% central collisions of Pb + Pb at  $\sqrt{s_{NN}} = 17$  GeV are also shown (closed triangles) [12]. Data at different beam energies are plotted as a function of the pseudo-rapidity shifted by the relevant beam rapidity. We note that the charged

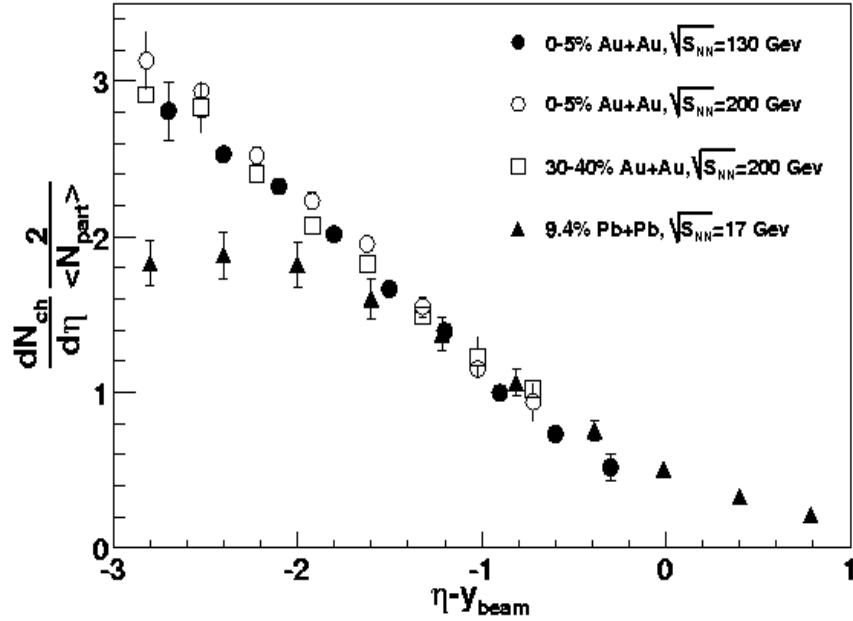


Figure 2

particle multiplicities in an interval up to 1.5 units below the beam rapidity are independent of the collision centrality and energy from  $\sqrt{s_{NN}} = 17$  GeV up to  $\sqrt{s_{NN}} = 200$  GeV. This observation is consistent with a limiting fragmentation picture in which the excitations of the fragment baryons saturate at moderate collision energies independently of system size [5]. In contrast, the charged particle multiplicities per participant pair increase with the center of mass energy in the region of the central rapidity, thus indicating that the increased energy results in an increase in particle production.

Figure 3 displays the dependence of the charged particle multiplicity per pair of participant baryons as a function of the number of participants for three narrow pseudo-rapidity regions ( $\Delta\eta \approx 0.2$ ) around  $\eta = 0, 3.0$  and  $4.5$ . The curves represent Kharzeev and Levin (solid line) and AMPT (dashed line) model calculations. We observe that particle production per participant pair is constant and close to unity in the fragmentation region (forward rapidities). However a significant increase of the particle production per pair of participant nucleons is seen for more central collisions at mid-rapidities. This rise has been attributed to the onset of hard scatterings processes which are dependent on the number of binary nucleon collisions,  $N_{coll}$ , rather than on the number of participant pairs,  $N_{part}$ . Using  $N_{coll}$  and  $N_{part}$  from HIJING we performed a phenomenological two component

analysis of the observed charged densities quoted in Table 1 to estimate the relative contributions of the soft and hard scattering components. We found that at  $\eta=0$ , the hard scattering component is almost constant at the two RHIC energies, with values of  $(20\pm 7)\%$  and  $(25\pm 7)\%$  at  $\sqrt{s_{NN}} = 130$  GeV and  $\sqrt{s_{NN}} = 200$  GeV, respectively. However, this simple analysis is highly model dependent.

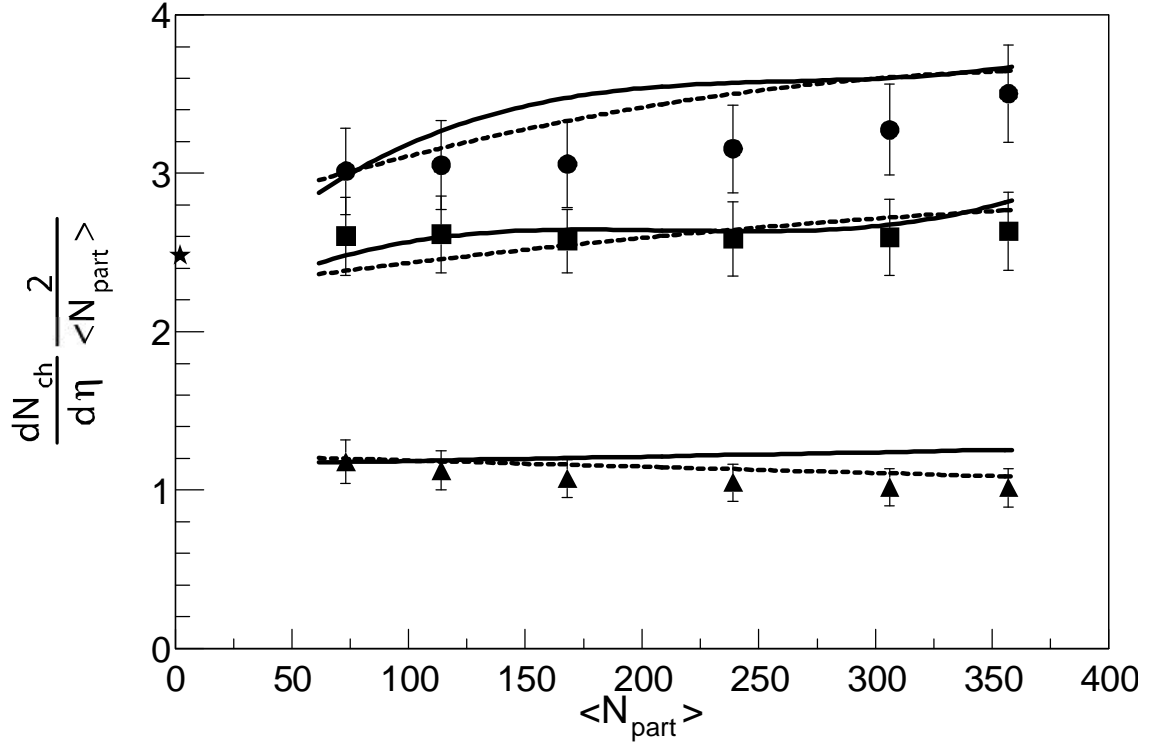


Figure 3.

The charged particle density in  $dN_{ch}/d\eta$  was also used to estimate so called Bjorken energy density,  $\epsilon_0$  [13]. The formula

$$\epsilon_0 = \frac{\langle p_t \rangle}{R^2 \tau_0} = \frac{3}{2} \frac{dN_{ch}}{d\eta}$$

provides the value of  $\epsilon_0 \approx 4$  GeV/fm<sup>3</sup> at  $\sqrt{s_{NN}} = 200$  GeV, where we assumed that  $\tau_0 = 1$  fm/c,  $\langle p_t \rangle = 0.5$  GeV/c and  $R = 6$  fm. This value is significantly above the energy density expected to result in quark-gluon plasma formation.

## 5. Conclusions

The BRAHMS experiments have measured pseudo-rapidity densities of

charged particles from  $^{197}\text{Au} + ^{197}\text{Au}$  collisions at  $\sqrt{s_{\text{NN}}} = 130 \text{ GeV}$  and  $\sqrt{s_{\text{NN}}} = 200 \text{ GeV}$ . The data were collected over a large range of pseudo-rapidities as a function of collision centrality. Although the full understanding of ultra-relativistic heavy ion collisions requires more detailed analyses, the current investigation leads to several conclusions:

- ?? The charged particle production scales smoothly from  $\sqrt{s_{\text{NN}}} = 130 \text{ GeV}$  to  $\sqrt{s_{\text{NN}}} = 200 \text{ GeV}$  in a wide region around midrapidity.
- ?? The charged particle multiplicities in the interval of approximately  $-0.5$  to  $-1.5$  units below the beam rapidity are largely independent of the collision centrality and collision energy, supporting a limiting fragmentation picture. In contrast, around the center of mass rapidity, an increase in the reaction energy is utilized for increased particle production.
- ?? The data are well reproduced by the AMPT/HIJING model and calculations based on high density QCD. On the other hand, the BRAHMS experimental data rule out the UrQMD model at RHIC energies.
- ?? The estimated value of the Bjorken energy density at  $\sqrt{s_{\text{NN}}} = 200 \text{ GeV}$  is several times higher than the critical value predicted for the quark-gluon plasma phase transition.

## 6. Acknowledgements

We thank the RHIC collider team for their efforts. This work was supported by the Division of Nuclear Physics of the U.S. Department of Energy, the Danish Natural Science Research Council, the Korea Research Foundation, the Research Council of Norway, the Polish State Committee for Scientific Research (KBN) and the Romanian Ministry of Research.

## 7. Reference

- [1] CERN Press Release Feb. 10, 2000:  
<http://cern.web.cern.ch/CERN/Announcements/2000/NewStateMatter/>
- [2] RHIC Design Manual. Technical Report, BNL:  
<http://www.rhichome.bnl.gov/NT-share/rhicdm>
- [3] D. Beavis et al., The BRAHMS Collaboration: “Conceptual Design Report for BRAHMS”, Report BNL-62018.  
<http://www.rhic.bnl.gov/brahms/WWW/cdr/cdr.html>
- [4] I. G. Bearden et al., Phys. Rev. Lett. **87** (2001) 112305-1.
- [5] I. G. Bearden et al., Phys. Lett. **B 523** (2001) 227; nucl-ex/0108016.
- [6] I. G. Bearden et al., nucl-ex /0112001 and submitted to Phys. Rev. Lett.
- [7] D. Ouerdane, in this volume.
- [8] X. Wang and M. Gyulassy, Phys. Rev. **D 44** (1991) 3501.
- [9] Zi-wie Lin, et al., Nucl. Phys. **A 698** (2002) 375c, nucl-th/0105044 and references quoted therein.
- [10] D. Kharzeev and E. Levin, nucl-th/0108006 and private communications.
- [11] S. A. Bass et al., Prog. Part. Nucl. Phys. **41** (1998) 255, nucl-th/983035.
- [12] P. Deines-Jones et al., Phys. Rev. **D 41** (2000) 014903.
- [13] J. D. Bjorken, Phys. Rev. **D 27** (1983) 140.